Earth and Planetary Science Letters 411 (2015) 72–86

Contents lists available at ScienceDirect

Earth and Planetary Science Letters

www.elsevier.com/locate/epsl

Rock-magnetic proxies of wind intensity and dust since 51,200 cal BP from lacustrine sediments of Laguna Potrok Aike, southeastern Patagonia

Agathe Lisé-Pronovost [a,b,*], Guillaume St-Onge [a,b], Claudia Gogorza [c], Torsten Haberzettl [d], Guillaume Jouve [b,e], Pierre Francus [b,e], Christian Ohlendorf [f], Catalina Gebhardt [g], Bernd Zolitschka [f], PASADO Science Team [1]

[a] *Institut des sciences de la mer de Rimouski (ISMER), Canada Research Chair in Marine Geology, Université du Québec à Rimouski, Rimouski, Canada*
[b] *GEOTOP Research Center, Montréal, Québec, Canada*
[c] *Centro de Investigaciones en Física e Ingeniería del Centro de la Provincia de Buenos Aires (CIFICEN-CONICET), Tandil, Argentina*
[d] *Physical Geography, Institute of Geography, Friedrich-Schiller-University Jena, Jena, Germany*
[e] *Centre Eau, Terre et Environnement, Institut National de la Recherche Scientifique, Québec, Québec, Canada*
[f] *GEOPOLAR, Institute of Geography, University of Bremen, Bremen, Germany*
[g] *Alfred Wegener Institute Helmholtz Centre of Polar and Marine Research, Bremerhaven, Germany*

ARTICLE INFO

Article history:
Received 29 April 2014
Received in revised form 31 October 2014
Accepted 6 November 2014
Available online 18 December 2014
Editor: J. Lynch-Stieglitz

Keywords:
rock magnetism
wind intensity
dust
lake sediment
PASADO
Southern Hemisphere westerly winds

ABSTRACT

The sedimentary archive from Laguna Potrok Aike is the only continuous record reaching back to the last Glacial period in continental southeastern Patagonia. Located in the path of the Southern Hemisphere westerly winds and in the source region of dust deposited in Antarctica during Glacial periods, southern Patagonia is a vantage point to reconstruct past changes in aeolian activity. Here we use high-resolution rock-magnetic and physical grain size data from site 2 of the International Continental scientific Drilling Program (ICDP) Potrok Aike maar lake Sediment Archive Drilling prOject (PASADO) in order to develop magnetic proxies of dust and wind intensity at 52°S since 51,200 cal BP. Rock-magnetic analysis indicates the magnetic mineral assemblage is dominated by detrital magnetite. Based on the estimated flux of magnetite to the lake and comparison with distal dust records from the Southern Ocean and Antarctica, k_{LF} is interpreted as a dust indicator in the dust source of southern Patagonia at the millennial time scale, when ferrimagnetic grain size and coercivity influence are minimal. Comparison to physical grain-size data indicates that the median destructive field of isothermal remanent magnetization (MDF_{IRM}) mostly reflects medium to coarse magnetite bearing silts typically transported by winds for short-term suspension. Comparison with wind-intensity proxies from the Southern Hemisphere during the last Glacial period and with regional records from Patagonia since the last deglaciation including marine, lacustrine and peat bog sediments as well as speleothems reveals similar variability with MDF_{IRM} up to the centennial time scale. MDF_{IRM} is interpreted as a wind-intensity proxy independent of moisture changes for southeastern Patagonia, with stronger winds capable of transporting coarser magnetite bearing silts to the lake.

1. Introduction

The Southern Hemisphere westerly winds (SWW) play an important role in ocean circulation and the global climate system (e.g., Anderson et al., 2009; Sijp and England, 2008; Toggweiler et al., 2006). Yet the latitudinal position and intensity of the SWW in the past remain an open question (Kohfeld et al., 2013). Patagonia is one of the five major dust producing regions of the globe (Roberts et al., 2011) and is of particular interest because it is the main source area for dust deposited in Antarctica during glacial cycles (Basile et al., 1997; Delmonte et al., 2010, 2004; Gaiero, 2007; Petit et al., 1999; Sugden et al., 2009). Dust emission is believed to be related to changes in environmental conditions and possibly wind intensity (e.g., Muhs, 2013; Basile et al., 1997; Sugden et al., 2009). Sugden et al. (2009) argued that Patagonian glacier discharge into outwash plains or proglacial lakes acted like an

* Corresponding author at: La Trobe University, Melbourne, Australia. Tel.: +61 03 9479 1392; fax: +61 3 9479 1881.
E-mail address: A.Lise-Pronovost@latrobe.edu.au (A. Lisé-Pronovost).
[1] http://www-icdp.icdp-online.org/front_content.php?idcat=1494.

http://dx.doi.org/10.1016/j.epsl.2014.11.007

on/off switch for dust deposition in Antarctica, hence providing evidence for environmental control on dust emission during the last glaciation. In contrast, there is to date no record of paleo-wind intensities extending beyond the Late Glacial in southern Patagonia, where the available records mainly reach back to the Holocene and deglacial periods (e.g., Villa-Martinez and Moreno, 2007; Björck et al., 2012; Lamy et al., 2010; Mayr et al., 2007a, 2013; Moreno et al., 2012, 2009; Waldmann et al., 2010). In order to fully address dust emission in southern Patagonia during the last Glacial and better constrain past changes in the SWW, paleo-wind intensity records from the source region of dust deposited in Antarctica are needed.

Paleo-wind indicators in southern Patagonia are commonly moisture proxies (e.g., pollen, paleo-fire history, lake level, and mineralogical data) assuming a major control of wind intensity on rainfall (Kilian and Lamy, 2012; Kohfeld et al., 2013). However on the eastern side of the Andes, precipitation is only weakly correlated to westerly wind strength because the very low precipitation mostly comes from the east and south–west (Garreaud et al., 2013) and evaporation strongly influences available moisture (Lamy et al., 2010; Moy et al., 2008; Ohlendorf et al., 2013). As a result, numerous moisture-related wind intensity proxies are difficult to interpret (Fletcher and Moreno, 2012; Moreno et al., 2009) and there is a need for different types of proxies.

The long sedimentary archive from Laguna Potrok Aike is the only continuous paleoenvironmental archive from this region reaching back to the last Glacial period (Kilian and Lamy, 2012; Zolitschka et al., 2013). Haberzettl et al. (2009) revealed that the millenial-scale variability of magnetic susceptibility measured on an independently dated short sediment core collected from low water depth corresponds to the non-sea-salt calcium (a dust proxy) from the Antarctic ice core EDC (Röthlisberger, 2002). Such comparison of magnetic susceptibility signal to dust record were also reported in sediments from the Southern Ocean and used to constrain chronologies (Pugh et al., 2009; Weber et al., 2012). Magnetic susceptibility documents how “magnetisable” the sediment is and while it often primarily reflects changes in the concentration of ferrimagnetic minerals, it can also be significantly influenced by dia-, antiferro-, para-, and superparamagnetic material when the concentration of ferrimagnetic mineral is low, as well as by changes in magnetic grain size (e.g., Dearing, 1999; Liu et al., 2012). Interpreting magnetic susceptibility records is therefore not straightforward and detailed rock-magnetic studies from Laguna Potrok Aike are necessary to investigate its environmental significance (Haberzettl et al., 2009; Maher, 2011). Here we use high-resolution rock-magnetic data from the sediment deposited in the deepest part of Laguna Potrok Aike in order to investigate what controls the magnetic susceptibility signal and develop a new proxy of wind intensity in southeastern Patagonia since 51,200 cal BP.

2. Geological setting

Laguna Potrok Aike (51°58′S, 70°23′W; 113 m a.s.l.) is a maar lake in the Pali Aike volcanic field of southern Argentina (Fig. 1A) containing a series of mass movement deposits associated with hydrological changes, major volcanic eruptions and possibly earthquakes (Anselmetti et al., 2009; Kliem et al., 2013a, 2013b). The maximum water depth is 100 m and the maximum diameter is 3.5 km (Haberzettl et al., 2005; Zolitschka et al., 2006). The lake is located in the mid-latitudes of the Southern Hemisphere, presently at the southern limit of the strong SWW belt, where winds can reach a monthly average speed of about 10 m/s at the beginning of the summer (Schäbitz et al., 2013). The lake is polymictic; there is currently no stratification and the water column is well oxygenated from top to bottom (Zolitschka et al., 2006). A recent high-resolution geochemical study revealed that such oxic conditions have predominated since 51,200 cal BP (Hahn et al., 2014). In addition, low primary productivity and low organic carbon fluxes likely prevented the development of strong redox gradients at the water-sediment interface (Nuttin et al., 2013), as also suggested by the infrequent authigenic mineral formation only associated to reworked sedimentation events (Vuillemin et al., 2013; Lisé-Pronovost et al., 2014). On the lee-side of the Andean Cordillera, the annual precipitation is low (ca. 200 mm/yr; Mayr et al., 2007b; Ohlendorf et al., 2013), the climate is semi-arid and the vegetation is characterized by a dry steppe (Schäbitz et al., 2013; Wille et al., 2007). Precipitation in this area mostly originates from moist Atlantic air masses at times of weaker SWW (Mayr et al., 2007b; Ohlendorf et al., 2013). There is currently no permanent surface inflow from the catchment area (200 km^2 in size) and no outflow (Haberzettl et al., 2005; Zolitschka et al., 2009). This geographical, climatic and geomorphological setting results in frequent sediment remobilization events in the lake (Kliem et al., 2013a) and suggests that detrital sediments are brought to the lake primarily by wind and subordinated by episodic runoff.

The surface geology of the region (Fig. 1B) is dominated by semi-consolidated sedimentary rocks of the Miocene Santa Cruz Formation (sandstone and siltstone) that are 660 m thick and extensively crop out around Laguna Potrok Aike (Coronato et al., 2013). Also present are Mio-Pliocene basalts and pyroclastic sediments, and unconsolidated Quaternary deposits including tills, glaciofluvial, fluvial, lacustrine and aeolian sediments (Coronato et al., 2013; D'Orazio et al., 2000; Ross et al., 2011; Zolitschka et al., 2006). Only minor modification to the overall landscape occurred since the phreatomagmatic formation of the maar in the Middle Pleistocene (Coronato et al., 2013; Zolitschka et al., 2013).

3. Methods

3.1. Coring and sampling

The international science team of the Potrok Aike maar lake Sediment Archive Drilling prOject (PASADO) cored the sediments of Laguna Potrok Aike in the framework of the International Continental scientific Drilling Program (ICDP) during austral spring 2008. The sedimentary infill of the maar was sampled up to a depth of ca. 100 m at two sites in the central basin using a hydraulic piston corer on the GLAD800 platform operated by DOSECC Inc.

Site 2 (Fig. 1A) was selected as the principal record for the multi-proxy PASADO paleoenvironmental studies because of higher core recovery and lower apparent sand content than site 1 (Zolitschka et al., 2009). The composite sedimentary sequence was established from three holes at site 2 and is 106.09 m long (Kliem et al., 2013a). It was continuously sampled for paleomagnetic and rock-magnetic analyses using u-channels (2 × 2 cm section plastic liner) and a series of discrete samples (2–3 g at ca. 40 cm intervals) at the University of Bremen in June 2009.

3.2. Rock-magnetic measurements

Rock-magnetic measurements on u-channel samples were performed at 1-cm intervals at the *Institut des sciences de la mer de Rimouski* (ISMER). Volumetric low field magnetic susceptibility (k_{LF}) was measured using a Bartington point sensor MS2E (high sensitivity surface measurement over 0.38 cm; Dearing, 1999) mounted on a GEOTEK Multi Sensor Core Logger (St-Onge et al., 2007). The anhysteretic remanent magnetization (ARM) was induced in a peak alternating field of 100 mT in the presence of a weak direct current (DC) biasing field of 0.05 mT using a 2G Enterprises ARM module. Isothermal remanent magnetization (IRM) was imparted using a 2G Enterprises pulse magnetizer in DC fields of 300 mT

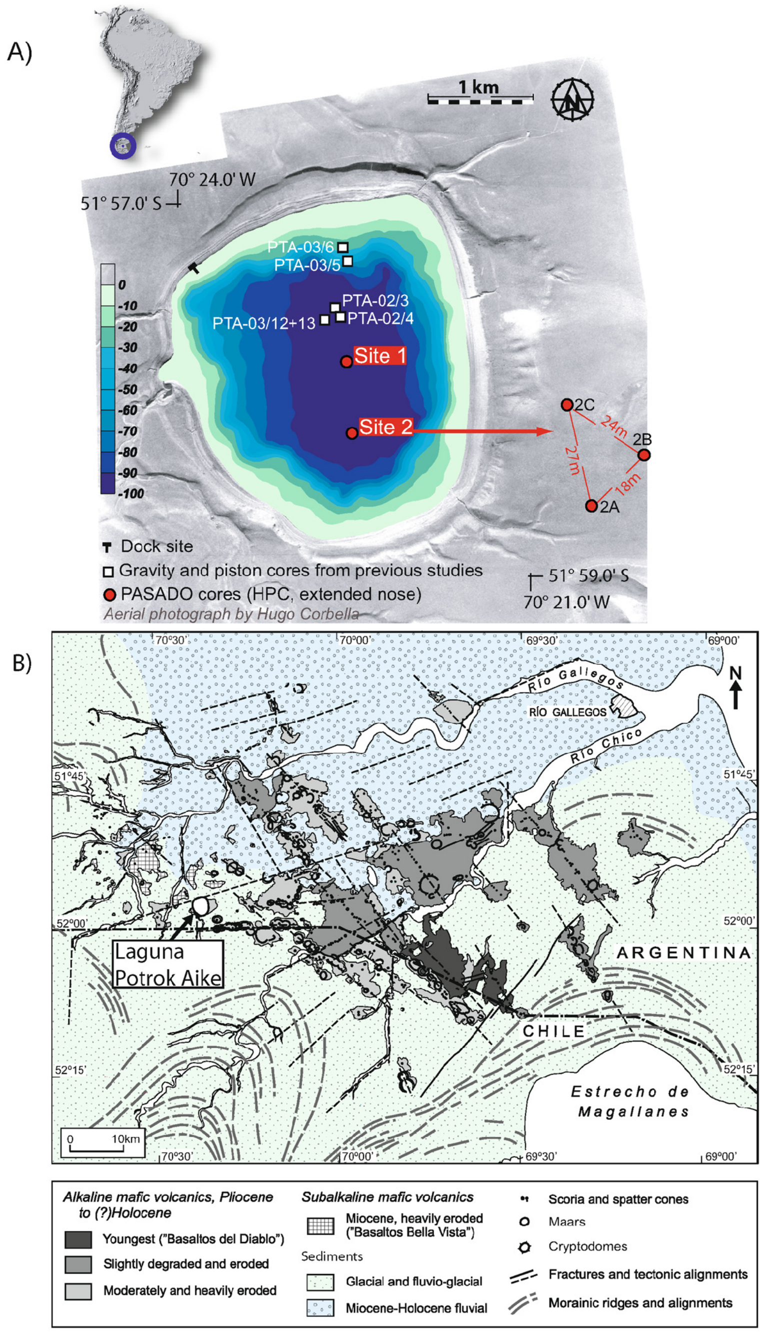

Fig. 1. A) Aerial photography and bathymetry from Laguna Potrok Aike in Southern Argentina. Position of the PASADO coring sites as well as cores from previous studies are indicated. B) Geological and geomorphological map of regional surface deposits in the Pali Aike Volcanic Field (modified from Ross et al., 2011).

and 950 mT. Each remanent magnetization was step-wise demagnetized and measured with a minimum of 8 steps (0, 10, 20, 30, 40, 50, 60, 70 mT) using a 2G Enterprises SRM-755 u-channel cryogenic magnetometer. The remanence measurement integrates over a distance of ca. 7–8 cm, as determined by the half-peak width of the magnetometer pick-up coils' response function. For comparison purposes between magnetic susceptibility and remanence data, as well as with other data from the PASADO site 2 sediment core, each dataset was interpolated at 10 years interval (initial average resolution of 11.34 years; Kliem et al., 2013a) and smoothed over 50 data points to obtain the millennial timescale variability. Both the raw data and the millennial time scale variability (gray and black curves, respectively) are represented in Figs. 3, 6 and 8.

ARM and IRM are primarily related to the concentration of ferrimagnetic grains and both also depend on the magnetic domain state, however in a different manner. Single domain (SD) grains more easily acquire an ARM than multi domain (MD) grains (Maher, 1988; Dunlop and Özdemir, 2007; Evans and Heller, 2003; King et al., 1982) and as a result, the smaller grains (<1 μm) will acquire more efficiently an ARM and the coarser grains (>10 μm and up to a few tens of μm) will acquire more efficiently an IRM (Stoner et al., 1996; Peters and Dekkers, 2003). The susceptibility of anhysteretic remanent magnetization (kARM) is calculated by dividing the ARM with the DC biasing field. kARM is a measure of the magnetic concentration and domain state and is commonly used as a magnetic grain size indicator when divided by magnetic susceptibility or IRM (e.g., kARM/k, kARM/IRM) (Egli, 2004; Maher, 1988; Evans and Heller, 2003; Stoner and St-Onge, 2007; Banerjee et al., 1981; King et al., 1982). The median destructive field (MDF) is the required field to demagnetize half of the initial

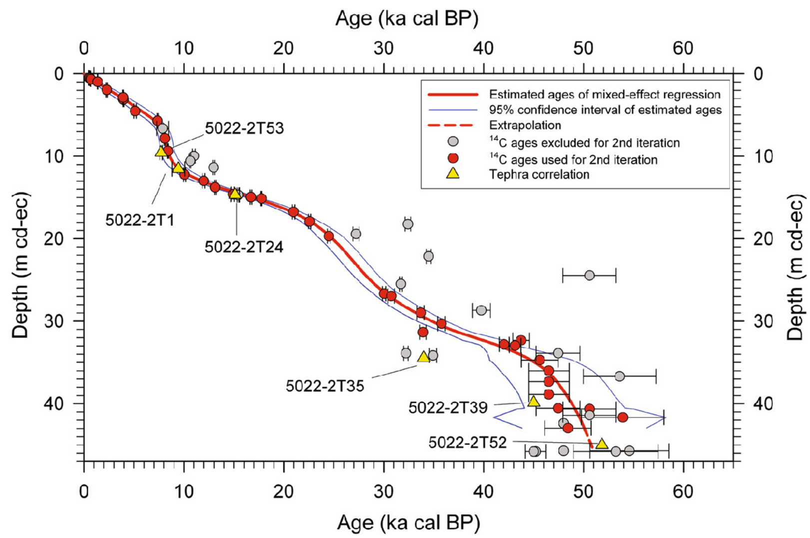

Fig. 2. Radiocarbon-based age model for site 2 of the PASADO sediment record (modified from Kliem et al., 2013a). Radiocarbon dates and tephra correlation are presented along the event-corrected composite depth (cd-ec) after removal of mass movement deposits. The red line is the estimated age after two iterations of mixed-effect regressions using the constant-variance function (for more details, see Kliem et al., 2013a). (For interpretation of the references to color in this figure legend, the reader is referred to the web version of this article.)

remanent magnetization of a sample and it represents the coercivity of the magnetic assemblage. Within uniform mineralogy MDF can reflect grain size, with coarser grains easier to demagnetize and thus displaying lower MDF values and vice-versa (Dankers, 1981; Dunlop and Özdemir, 1997). The ratio of the MDF of the ARM normalized by the MDF of the IRM (MDF_{ARM}/MDF_{IRM}) is notably used in the Lowrie–Fuller test (Lowrie and Fuller, 1971) to inform on the coercivity distribution and indirectly on the magnetic domain state and grain size of a sample (Xu and Dunlop, 1995; Dunlop and Özdemir, 1997).

Rock-magnetic measurements on 103 discrete samples from the pelagic sediment sequence were performed using a Princeton Measurement Corporation alternating gradient force magnetometer (model MicroMag 2900 AGM) in maximum field of 300 mT in order to obtain the bulk coercive force (Hc), the remanent coercive force (Hcr), the saturation magnetization (Ms) and the saturation remanence (Mr). The ratios Hcr/Hc and Mr/Ms are commonly used in a Day plot (Day et al., 1977; Dunlop, 2002) to estimate the domain state of the magnetic assemblage.

Estimation of the magnetite flux (Fmag) to the coring site is calculated (see below) in order to evaluate if concentration changes primarily control the k_{LF} record. If this is the case, one would expect Fmag to mimic k_{LF} variability. This simple test is adequate for the sediments of Laguna Potrok Aike because the magnetic assemblage in the pelagic sediments is dominated by magnetite (Section 4.1; Gogorza et al., 2012, 2011; Lisé-Pronovost et al., 2013, 2014; Recasens et al., 2012). Following the method previously used by Mazaud et al. (2010, 2007), Fmag is calculated with Eq. (1) using the volumetric low field magnetic susceptibility (k_{LF}), the sedimentation rate derived from the radiocarbon-based chronology (sedrate; Kliem et al., 2013a) and a theoretical mass specific magnetic susceptibility value of 5.96×10^{-3} $m^3\,kg^{-1}$ for magnetite (Kmag) (Dearing, 1999).

$$\mathrm{Fmag} = (k_{LF}/\mathrm{Kmag}) \times \mathrm{sedrate} \tag{1}$$

3.3. Physical grain size measurement

Physical grain size measurements were conducted at ca. 8-cm intervals at the University of Bremen. Freeze-dried and homogenized samples were pre-treated with 5% NaClO over 4 days to remove organic material. The sediment was then washed with demineralized water until a pH of 7–8 was reached, and charged with a (calgon) solution of 35 g Hexametaphosphate and 7 g Na-carbonate in 1 liter of demineralized water some 24 h before measurements were carried out in order to prevent flocculation of particles. Grain-size analyses were performed using a laser diffraction particle size analyzer (LS 200, Beckman Coulter) equipped with a variable-speed fluid module which measures particles from 0.4 to 2000 μm. At least 5 measurements were taken per sample, and the arithmetic average of all stable runs was used for further calculation. The Fraunhofer optical model was applied to calculate the grain size distribution.

3.4. Lithology

Five lithological units were described for the composite sediment record (106.09 m cd) of Laguna Potrok Aike reaching back to 51,200 cal BP (Kliem et al., 2013a). The units are based on the type of pelagic sediment and the frequency of mass movement deposits (MMD) and include: (A) pelagic laminated silts, (B) pelagic laminated silts intercalated with thin fine sand and coarse silt layers, (C) alternation of A and B with an increase in the frequency and thickness of MMD from C-1 to C-3 (see stratigraphy and lithology in Fig. 4). MMD are expressed as ball and pillow structures, normally graded beds, structureless sand and fine gravel layers, matrix supported layers and one folded sediment structure (Kliem et al., 2013a). Here we present results from the event-corrected composite depth (45.8 m cd-ec), comprising pelagic sediment only, deposited at an average rate of 80 cm ka^{-1} (207 cm ka^{-1} with MMDs included; Kliem et al., 2013a). The MMDs are therefore excluded from the stratigraphic record presented in this paper and are discussed elsewhere (Kliem et al., 2013a, 2013b; Lisé-Pronovost et al., 2014).

3.5. Chronology

The chronology of the PASADO site 2 pelagic sediment sequence is based on 58 radiocarbon dates and the age model was built using a mixed-effect regression procedure (Kliem et al., 2013a) (Fig. 2). The age model is supported by lithological and tephra correlation with previously studied cores from Laguna Potrok Aike, including a core located nearby in the lake

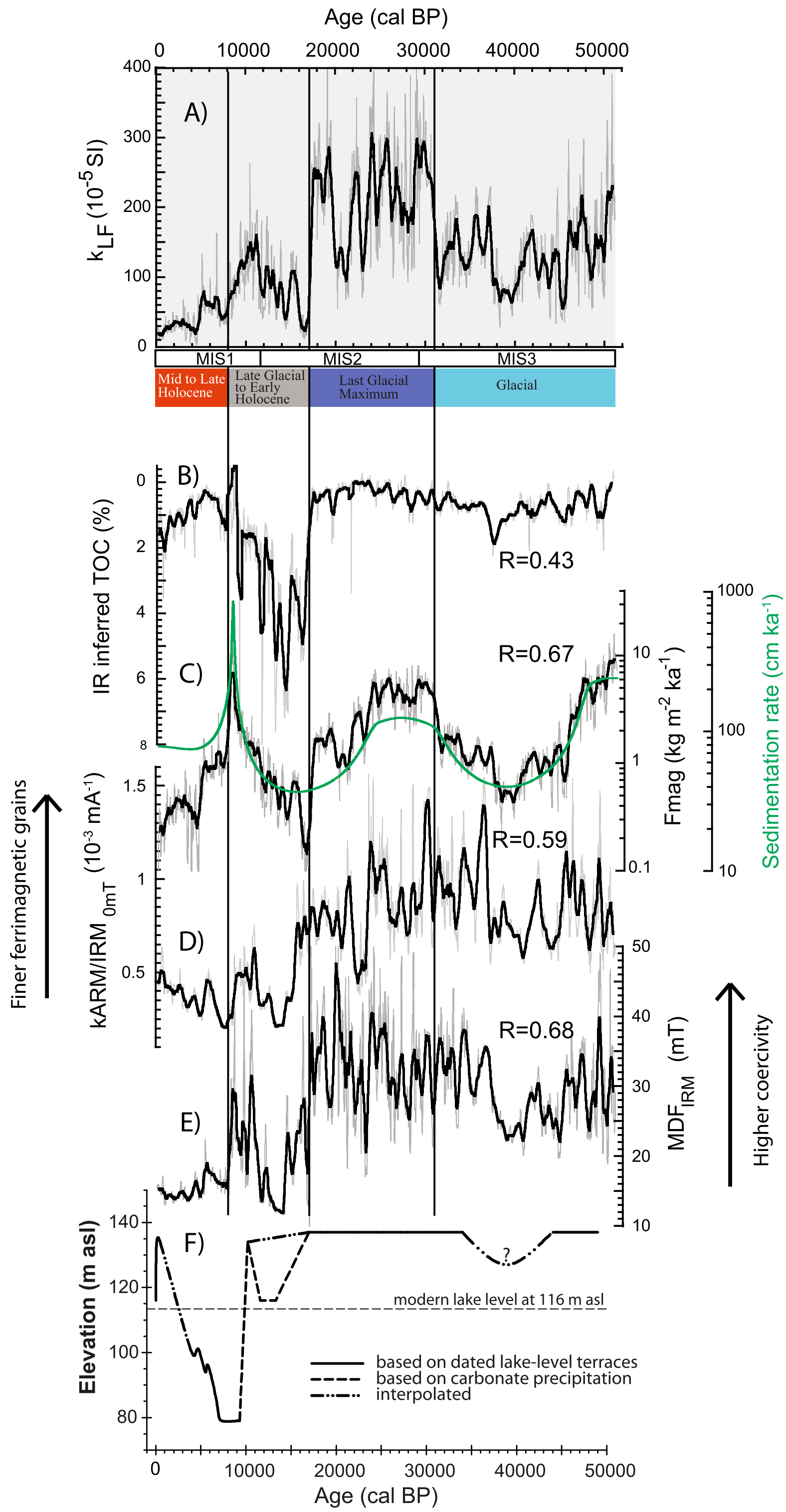

Fig. 3. A) Low field volumetric magnetic susceptibility record (k_{LF}) from Laguna Potrok Aike compared with B) infrared inferred total organic carbon (IR inferred TOC; Hahn et al., 2013), C) calculated flux of magnetite to the lake floor (Fmag) and sedimentation rates (Kliem et al., 2013a), D) kARM/IRM$_{0\,mT}$ ratio, E) median destructive field of isothermal remanent magnetization (MDF$_{IRM}$) and F) lake-level reconstruction (Zolitschka et al., 2013). Each rock-magnetic parameter was interpolated to 10 years interval (initial average resolution of 11.34 years; Kliem et al., 2013a) and smoothed over 50 data points in order to obtain the millennial time scale variability. For each parameter the linear correlation coefficient (r for $n = 5066$) with k_{LF} is indicated. Climatic periods inferred from rock-magnetic parameters and previous sedimentological studies from Laguna Potrok Aike (Hahn et al., 2013; Kliem et al., 2013a) as well as marine isotopic stages (MIS) according to Lisiecki and Raymo (2005) are indicated.

center and covering the last 16,000 cal BP (PTA03/12+13; location in Fig. 1A; Haberzettl et al., 2007) and a low-resolution core from a submerged lake level terrace reaching back to the last Glacial period (PTA03/5+6; location in Fig. 1A; Haberzettl et al., 2009). The age uncertainty is larger at the base of the record because of the increased occurrence of MMD and because the age approaches the limit of radiocarbon dating. Nonetheless, magnetostratigraphy using the relative paleointensity record supports the chronology in this problematic interval (Kliem et al., 2013a; Lisé-Pronovost et al., 2013).

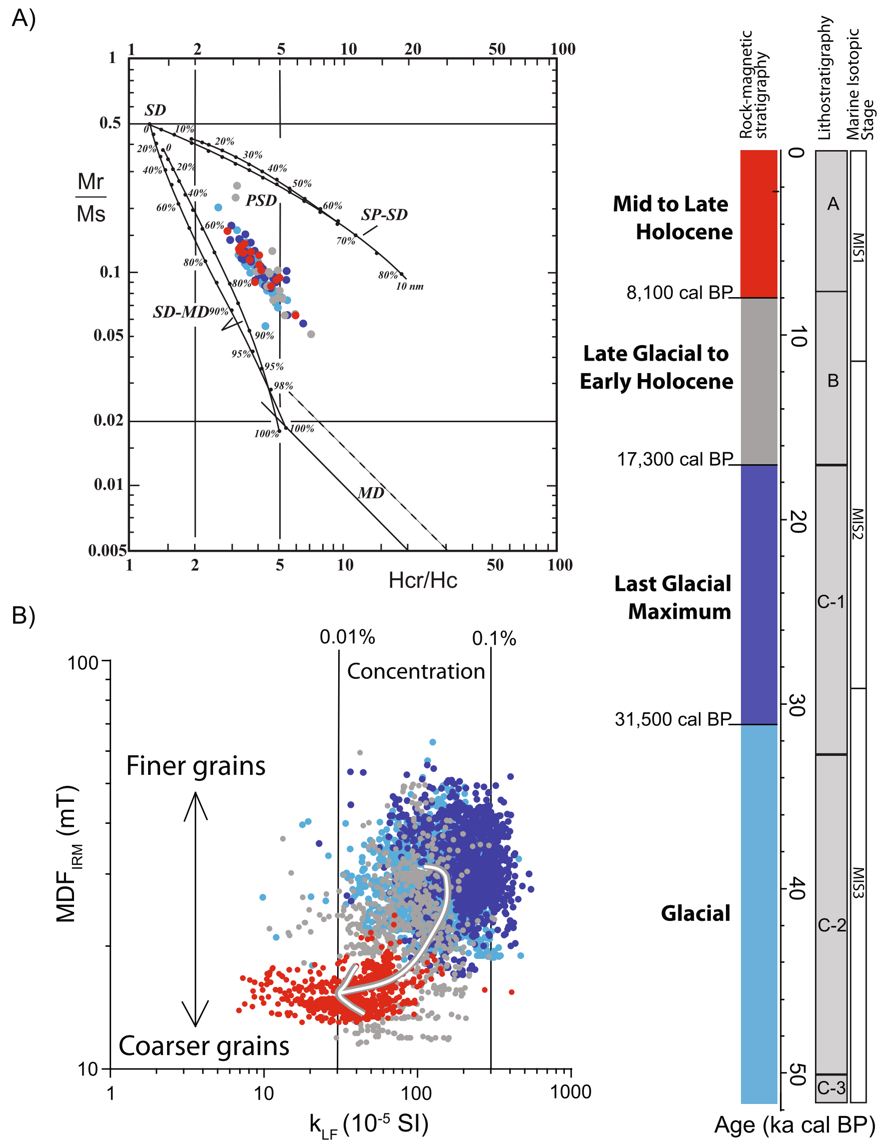

Fig. 4. A) Day plot diagram (Day et al., 1977) with mixing reference lines from Dunlop (2002) for pelagic sediment samples from Laguna Potrok Aike. B) Biplot of low field volumetric magnetic susceptibility (k_{LF}) with the median destructive field of isothermal remanent magnetization (MDF_{IRM}). The white arrow indicates the chronological change since 51,200 cal BP. Volumetric concentration of ferrimagnetic material is estimated from the k_{LF} values (Thompson, 1986) and indicated as vertical lines. Data from different climatic periods are color-coded. Marine isotopic stages (MIS) according to Lisiecki and Raymo (2005) and the simplified lithostratigraphic log from Kliem et al. (2013a) are also shown.

4. Results

4.1. Magnetic mineralogy

The first rock-magnetic and paleomagnetic-dedicated studies from Laguna Potrok Aike were published as part of the South Argentinean Lake Sediment Archives (SALSA) project (past 16,000 cal BP; Gogorza et al., 2011; 2012; Irurzun et al., 2014) and the ICDP–PASADO project (past 51,200 cal BP; Recasens et al., 2012; Lisé-Pronovost et al., 2013, 2014). Altogether these studies clearly identified magnetite as the dominant magnetic carrier as indicated by temperature-dependent magnetic susceptibility, thermal demagnetization after induction of a saturating field, step-wise acquisition of IRM in field up to 2.5 T, s-ratio ($IRM_{300\,mT}/IRM_{1200\,mT}$), soft-IRM ($IRM_{-40\,mT}/IRM_{1200\,mT}$), the shape of the hysteresis loop, the remanent coercive field (Bcr) and X-ray diffraction analyses of magnetic extracts. Other magnetic minerals than magnetite were only identified in specific intervals, and include greigite (Vuillemin et al., 2013; Jouve et al., 2013; Lisé-Pronovost et al., 2014; Irurzun et al., 2014), hematite and/or goethite (Lisé-Pronovost et al., 2014), and possibly maghemite (Gogorza et al., 2012; Lisé-Pronovost et al., 2014). These intervals represent a total of ca. 5% of the PASADO composite sediment sequence at site 2 and occur in association with mass movement deposits (Lisé-Pronovost et al., 2014), which were removed from the event-corrected pelagic sediment sequence (Kliem et al., 2013a) presented in this paper. While magnetite clearly predominates in the pelagic sediment and held genuine paleomagnetic records (Gogorza et al., 2012; Lisé-Pronovost et al., 2013), minor contribution of other ferrimagnetic minerals such as titanomagnetite and/or maghemite is suggested by subtle change in the magnetic susceptibility slope of some of the heating curves at 200–350 °C (Recasens et al., 2012; Gogorza et al., 2012; Lisé-Pronovost et al., 2013), as well as data slightly shifted to the right of the theoretical mixing line for magnetite in a Day plot (Fig. 4A; Recasens et al., 2012; Lisé-Pronovost et al., 2013). However, the latter could also be attributed to a superparamagnetic contribution. The magnetic mineralogy of the pelagic sediment possibly includes small quantities of oxidized and/or ti-substituted magnetite and/or superparamagnetic grains together with the dominant mineral magnetite.

4.2. Rock-magnetic stratigraphy

Based on rock magnetic variability as defined by k_{LF}, MDF_{IRM} and kARM/IRM, four main units stand out (Fig. 3). When placed on time these units are: from the base of the record (51,200 cal BP) to 31,500 cal BP, 31,500–17,300 cal BP, 17,300–8100 cal BP and 8100–0 cal BP. These rock-magnetic units are in general agreement with the lithostratigraphic units described by Kliem et al. (2013a) (see logs Fig. 4) and interpreted as the Glacial period (C-3/2), the Last Glacial Maximum (LGM; C-1), the Late Glacial to early Holocene (B) and the mid to late Holocene (A) (Hahn et al., 2013; Kliem et al., 2013a).

The units forming the base of the record (51,200 cal BP) to 17,300 cal BP correspond to the Last Glacial period. They are characterized by finer magnetic grains than the other units, as indicated by the kARM/IRM ratio and MDF_{IRM} (Fig. 3D–E). The LGM is delimited by a sharp change to higher values of k_{LF} at 31,500 cal BP and a sharp decrease at 17,300 cal BP (Fig. 3A), also present in other bulk ferrimagnetic concentration parameters (ARM and IRM, cf. Lisé-Pronovost et al., 2013) but absent in magnetic grain size indicators (kARM/IRM and MDF_{IRM}; Fig. 3D–E). The late Glacial to early Holocene period (17,300–8100 cal BP) presents intermediate values of magnetic grain size and concentration proxies, with relatively high amplitude of change (Figs. 3 and 4). The organic content in the sediments of Laguna Potrok Aike abruptly increases (Fig. 3B; Hahn et al., 2013) at the onset of deglaciation in the mid-latitudes of the Southern Hemisphere (17,300 cal BP; Schaefer et al., 2006). This dilutes the detrital input with less magnetic grains. Thus, the concentration-dependent parameters such as k_{LF} and the calculated Fmag decrease concomitantly (Fig. 3A and C). Finally, the Mid- to Late Holocene unit (since 8100 cal BP) is characterized by distinctively lower MDF_{IRM} values (Figs. 3E and 4B). This sharp change in coercivity could possibly reflect a shift in ferrimagnetic mineralogy (degree of oxidation and/or ti-substitution of magnetite; Dunlop and Özdemir, 2007), strongly interacting single domain (SD) particles (Cisowski, 1981; Dunlop and Özdemir, 1997), and/or a shift towards distinctively coarser magnetite grains acquiring the IRM. The former is unlikely considering the magnetic mineralogy is virtually uniform in the pelagic sediments of the PASADO record, without any sharp change (Lisé-Pronovost et al., 2013, 2014). In addition, analysis of the IRM acquisition curve (Supplementary material 1; Kruiver et al., 2001) for representative samples shown in Fig. 5 clearly indicates one Gaussian coercivity distribution and further points to an essentially monomineralic magnetic mineralogy dominated by magnetite. Magnetic interaction of SD particles could influence MDF values. However the domain states of Laguna Potrok Aike sediments are in the PSD-MD range (and not in the SD range; Fig. 4A), as also indicated by narrow hysteresis curves, first-order reversal curve diagram (Lisé-Pronovost et al., 2013, 2014), steep IRM acquisition and demagnetization curves at low field values (Fig. 5), and median MDF_{ARM}/MDF_{IRM} value of 0.83 (values <1 indicate MD-type magnetite; Xu and Dunlop, 1995), altogether indicating no magnetic interaction. Moreover, unchanged average domain state for the total magnetic assemblage since 51,200 cal BP (Fig. 4A) indicates that the sharp coercivity change at 8100 cal BP does not affect the entire grain size range of pseudo-single domain state (typically 0.1–20 μm; Moskowitz, 1991; Dunlop and Özdemir, 1997), but is specific to the fraction more efficiently acquiring IRM (mostly >10 μm; Fig. 4B).

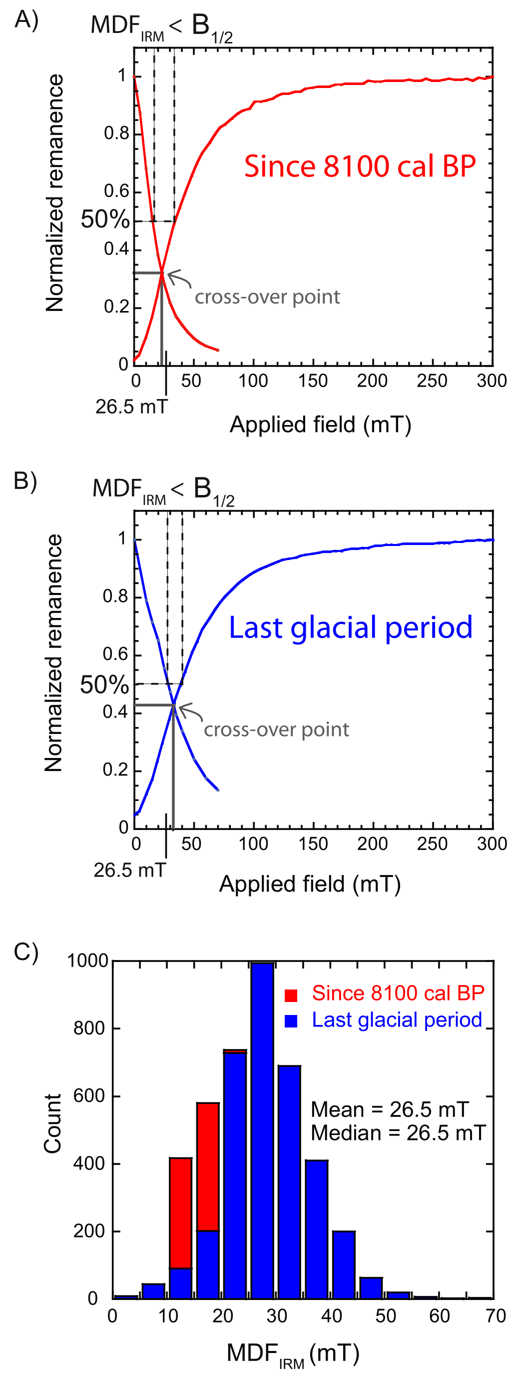

Fig. 5. Isothermal remanent magnetization (IRM) acquisition up to 300 mT and alternating field (AF) demagnetization after induction of $IRM_{950\,mT}$ (same as for $IRM_{300\,mT}$) for A) representative sediment for the period since 8100 cal BP (48 cm cd; 560 cal BP) and B) representative sediment for the last glacial period (3252 cm cd; 27,720 cal BP). IRM acquisition was conducted on discrete samples and AF demagnetization was conducted on u-channel samples. MDF_{IRM} value (50% of AF demagnetization) lower than $B_{1/2}$ value (50% of IRM acquisition) is typical of magnetite (Dankers, 1981) and steep exponential-like curves at low fields are typical of multi domain (MD) particles and indicate no magnetic interaction (Cisowski, 1981; Dunlop and Ozdemir, 1997). The lower cross-over point during the period since 8100 cal BP suggests an increased contribution of MD magnetite during that period. C) Frequency histogram for MDF_{IRM}.

4.3. Control on magnetic susceptibility

As stated earlier, the magnetic susceptibility of sediments is primarily influenced by the concentration of ferrimagnetic minerals, and also related to sediment composition, magnetic mineralogy and grain size (Dearing, 1999). The magnetic assemblage of the pelagic sediment is dominated by the ferrimagnetic mineral magnetite (Gogorza et al., 2011, 2012; Recasens et al., 2012; Lisé-Pronovost et al., 2013, 2014; Irurzun et al., 2014) which is up to two order of magnitude more magnetic than iron sulfides and up to four orders of magnitude more magnetic than antiferromagnetic minerals (such as hematite and goethite), or paramagnetic compounds such as clays (Dearing, 1999; Maher and Thompson, 1999). Therefore it is reasonably assumed that k_{LF} record from Laguna Potrok Aike reflects changes in 1) concentration and 2) grain size of magnetite, rather than mineralogical changes.

4.3.1. *Concentration of magnetite*

The change in concentration of magnetic minerals is estimated with the flux of magnetite (Fmag) to the lake (Fig. 3C). Fig. 3A and C reveal that the sedimentation rate and Fmag on log scales follow the multi-millennial time scale trends of k_{LF} ($r = 0.67$). The similar variability of sedimentation rate and k_{LF} using log scales points to aeolian transport of detrital magnetite to Laguna Potrok Aike because the transport of particles by wind is an exponential function of wind velocity (e.g., Pye, 1995; Maher et al., 2010). This observation also reveals that change in flux of magnetite drives the multi-millennial time scale variability in k_{LF}. However, high amplitude changes in k_{LF} at the millennial- to centennial time scale are not reproduced in Fmag, notably during the last Glacial period (before 17,300 cal BP; Fig. 3). This is likely the result of chronological smoothing (sedrate in Eq. (1)) and might also point to an influence of magnetic grain size on k_{LF} at the millennial to centennial time scale.

4.3.2. *Grain size of magnetite*

Previous studies investigating the influence of the physical grain size of magnetite on magnetic susceptibility overall suggest that there is no predicable relationship between these two parameters for the grain size range 0.09–6000 μm (Brachfeld, 1999 and references therein; Dearing, 1999; Tauxe, 2010; Dunlop and Özdemir, 2007; Heider et al., 1996). At Laguna Potrok Aike, the magnetic grain size indicator kARM/IRM and coercivity indicator MDF_{IRM} reveal that finer magnetic grain sizes moderately and strongly correlate ($r = 0.59$ and 0.68; Fig. 3D and E) with higher magnetic susceptibilities (cf., Lisé-Pronovost et al., 2013). The fact that neither MDF_{NRM} nor MDF_{ARM} correlate with k_{LF} ($r = 0.05$ and 0.03, respectively) indicates that only the grain size fraction > ca. 10 μm (those predominantly acquiring IRM; e.g., Stoner et al., 1996) correlate with k_{LF}. MDF_{IRM} displays the strongest correlation to k_{LF} and its millennial to centennial time scale amplitude variability resembles that of k_{LF} (Fig. 3A and E). This is supported by a coherence analysis using the Analyseries software (Paillard et al., 1996) between the two rock-magnetic parameters indicating that MDF_{IRM} and k_{LF} are coherent at the millennial to centennial time scale (periods less than 135 yr and periods centered at ca. 170, 195, 250 and 500; Supplementary material 2).

A closer look at the correlation between magnetic susceptibility and the coercivity indicator MDF_{IRM} with physical grain size reveals that the coarse to medium silt fractions hold most of the rock-magnetic information (Table 1). This sediment fraction is typical of loess deposits and more specifically of short-term aeolian transport in near-surface to low suspension clouds (Vandenberghe, 2013 and references therein). Coarse to medium silt-sized grains are also slightly finer than the first siliciclastic fraction moved by winds (Hjulström, 1935; Tucker, 2001), probably as a result of magnetite having higher density (5.1 g/cm^3) than the average siliciclastic sediments (e.g., quartz is 2.7 g/cm^3) from which the Hjulström curve is derived. The presence of magnetite inclusions within coarse to medium silt-sized siliciclastic host grains is also likely, as quartz and feldspar were present in magnetic extracts and identified using X-ray diffraction together with magnetite (Lisé-Pronovost et al., 2013). Altogether, the rock-magnetic and physical grain size data from the sediment of Laguna Potrok Aike reveal a similar variability of k_{LF} and MDF_{IRM} at the millennial to centennial time scale attributable to silt-sized (ca. 10–30 μm; Table 1) ferrimagnetic grains and/or inclusions within host grains transported to the lake by short-term suspension. The data presented in this paper is publicly accessible from the PANGAEA depository (http://doi.pangaea.de/10.1594/PANGAEA.837595).

Table 1
Linear correlation coefficient (r) of the physical grain size classes with the median destructive field of isothermal remanent magnetization (MDF_{IRM}) and magnetic susceptibility (k_{LF}). Data were interpolated in 10 years intervals and smoothed over 50 points in order to obtain the millennial time scale variability and to calculate r on a common scale ($n = 5066$). Both rock-magnetic parameters are best correlated to the coarse to medium silt fraction.

Physical grain size[a]		MDF_{IRM}	k_{LF}
Class	(μm)		
Total sediment		0.26	0.36
Fine sand	125–250	0.11	0.25
Very fine sand	63–125	0.40	0.45
Very coarse silt	31–63	0.039	0.14
Coarse silt	**16–31**	**−0.66**	**−0.59**
Medium silt	**8–16**	**−0.53**	**−0.56**
Fine silt	4–8	−0.27	−0.37
Very fine silt	2–4	−0.05	−0.18
Clay	<2	0.21	0.06

[a] The grain size intervals are from Udden (1914) and Wentworth (1922).

5. Discussion

5.1. *Interpretation of magnetic susceptibility*

Higher amount of magnetite grains brought to the lake during the Last Glacial can possibly be attributed to the activation of a source richer in detrital magnetite and/or a larger surface of erodible land such as outwash plains (Sugden et al., 2009), increased runoff due to permafrost (Kliem et al., 2013b), and/or enhanced gustiness of winds (McGee et al., 2010) capable of transporting more detrital magnetite to the lake. However, interpretation of the magnetic susceptibility signal is complicated by its correlation to ferrimagnetic grain size and coercivity (Fig. 3A, D and E), indicating that k_{LF} does not only reflect the amount of magnetite brought to the lake. As k_{LF} is largely independent of magnetite grain size except for ultrafine superparamagnetic particles (SP magnetite <0.03 μm; Dunlop and Özdemir, 1997), the results hint to possible SP contribution (undetectable at room-temperature; Gogorza et al., 2012; Lisé-Pronovost et al., 2014) occurring along with and/or as inclusion within silts, the physical grain size displaying correlation with k_{LF} and MDF_{IRM}. In addition, although believed to be small based on previous magnetic mineral studies at Laguna Potrok Aike (see Section 4.1), increased Ti substitution and/or oxidation from magnetite to maghemite by weathering could also influence k_{LF} and coercivity values (Dunlop and Özdemir, 1997). Hence interpreting the k_{LF} signal from Laguna Potrok Aike is not straightforward because of the complex control of ferrimagnetic grain concentration, size and coercivity.

Nevertheless, comparison of the high-resolution k_{LF} record from Laguna Potrok Aike with the flux of dust to the Dome C ice core, Antarctica (Lambert et al., 2012) (Fig. 6A and C) reveals a similar multi-millennial variability during the last Glacial period, as was first pointed out by Haberzettl et al. (2009) using a low resolution record from a submerged lake level terrace (core PTA-03\5-6; location in Fig. 1). Fig. 6B also presents the magnetic susceptibility of a marine core in the Scotia Sea interpreted as a distal dust record from southern Patagonia (Weber et al., 2012).

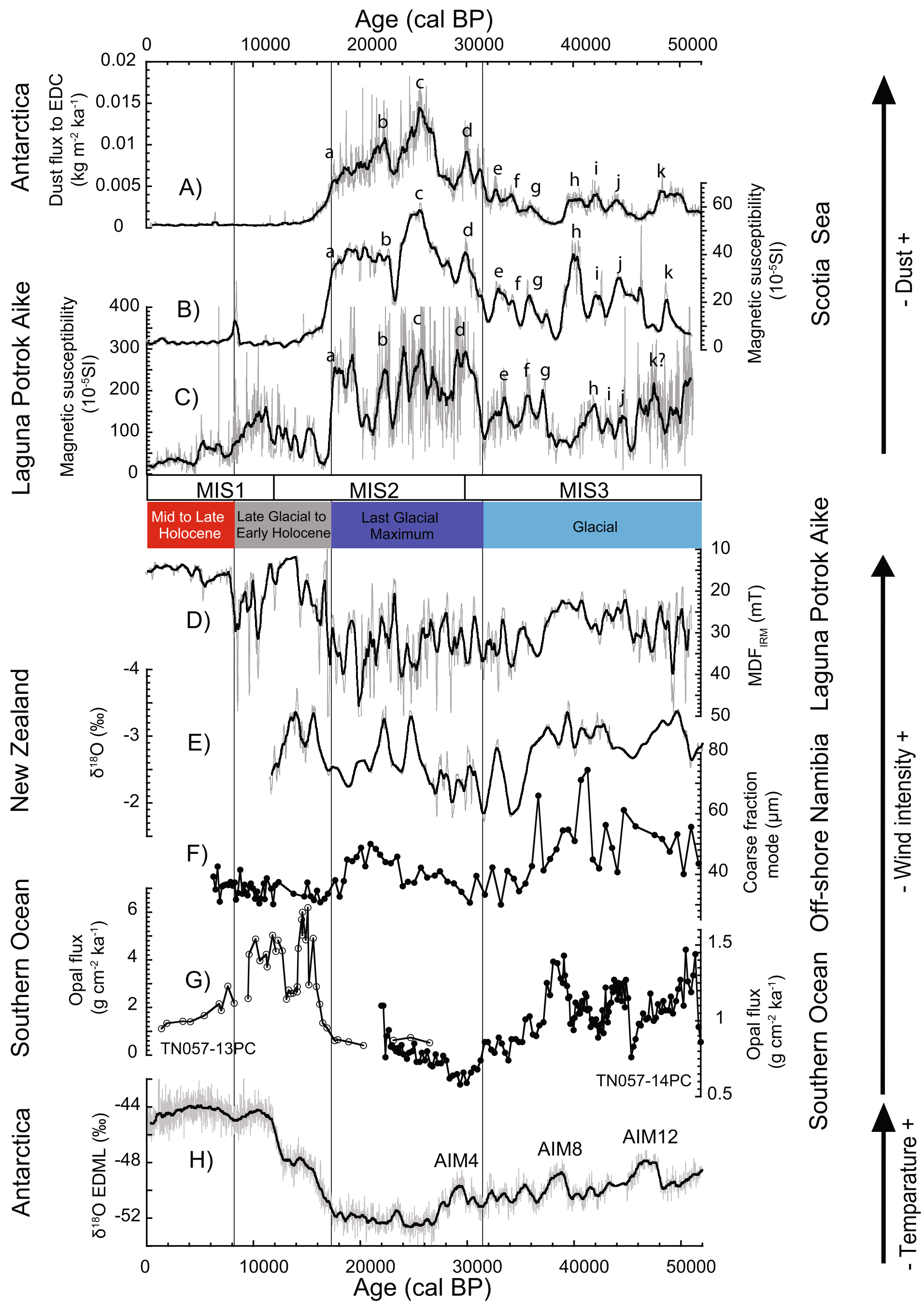

Fig. 6. Comparison of Southern Hemisphere dust, wind and temperature proxies since 52,000 cal BP (Table 2). From top to bottom: A) dust flux to EPICA Dome C (EDC) ice core in Antarctica (Lambert et al., 2012), B) magnetic susceptibility from the Scotia Sea (Weber et al., 2012), C) magnetic susceptibility from Laguna Potrok Aike (this study), D) median destructive field of isothermal remanent magnetization (MDF_{IRM}) from Laguna Potrok Aike (this study), E) $\delta^{18}O$ record from a speleothem in New Zealand (Whittaker et al., 2011), F) upwelling intensity off-shore Namibia from the coarse fraction mode of marine sediments (Pichevin et al., 2005), G) wind-driven upwelling intensity from opal flux in the Southern Ocean (Anderson et al., 2009) and H) paleo-temperature proxy $\delta^{18}O$ from EPICA Dronning Maud Land (EDML) ice core in Antarctica (EPICA Community Members, 2006). All records are presented on their own chronology. Thick lines represent the millennial-scale variability of high-resolution records A, B, C, D, E and H. Lowercase letters indicate dust maxima in A, B and C. Climatic periods from the PASADO record (Figs. 3 and 4; Kliem et al., 2013a; Hahn et al., 2013) and marine isotopic stages (MIS) according to Lisiecki and Raymo (2005) are indicated.

All records are smoothed to common millennial-scale variability for comparison purposes (thick lines, Fig. 6). The fluctuations from 51,200 to 17,300 cal BP can be correlated among the three records within the limit of their individual chronologies and common peak values are indicated with lowercase letters in Fig. 6A, B and C. In particular, all records display large amplitude changes at 31,500 cal BP (before feature *d*) and at 17,300 cal BP (after feature *a*) also observed in the estimated flux of magnetite to Laguna Potrok Aike (Fmag; Fig. 3C), thus hinting at a common environmental control on dust emission. However, at higher resolution (the millennial to centennial time scale variability) the distal records from Scotia Sea and Antarctica (Lambert et al., 2012; Weber et al., 2012) are not consistent with k_{LF} from Laguna Potrok Aike. Rock-magnetic and physical grain size results reveal that this difference is likely due to the influence of ferrimagnetic grain size and coercivity on k_{LF} at Laguna Potrok Aike. While proximal lacustro-aeolian records such as Laguna Potrok Aike accumulate grains transported by saltation and short-term

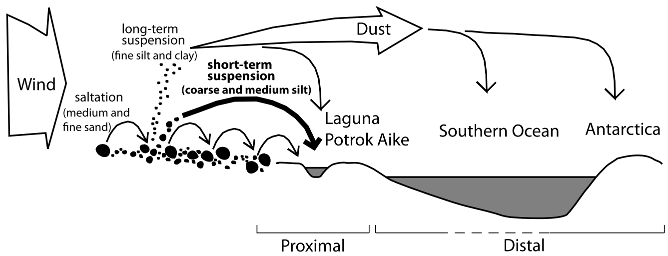

Fig. 7. Scheme of wind-induced transport processes for different grain sizes (modified from Pye, 1995) illustrating that while distal dust records (e.g., Southern Ocean and Antarctica) only contain fine particles, proximal records such as Laguna Potrok Aike are influenced by grain size changes. Medium to fine sands are transported by saltation (cm to m distance) and the impact of saltating grains on the ground results in short-term suspension of coarse to medium silts (traveling tens to hundreds of km distance) and long-term suspension of fine silt and clay (thousands of km distance). The thick arrow represents the transport process and the physical grain size best correlated to MDF_{IRM}.

suspension (Vandenberghe, 2013), distal dust records do not reflect grain-size changes because the size distribution of aerosols (grain sizes generally <10 μm traveling long distances; Muhs, 2013; Maher et al., 2010) is independent of wind intensity (Kok, 2011) (Fig. 7). Consequently, the magnetic susceptibility signal from Laguna Potrok Aike is interpreted as a dust indicator from southern Patagonia uniquely at multi-millennial resolution, where the ferrimagnetic grain size and coercivity influence is minimal.

5.2. *Rock-magnetic proxy of wind intensity*

5.2.1. *Physical processes*

The coercivity of magnetic grains acquiring an IRM (MDF_{IRM}) is best correlated ($R = -0.66$ and $R = -0.53$) to coarse and medium silt fractions (31–16 μm and 16–8 μm, respectively; Table 1) corresponding to the grain-size fraction lifted by winds but unlikely to travel long distances (Muhs, 2013; Vandenberghe, 2013; Maher et al., 2010 and references therein) (Fig. 7). Coronato et al. (2013) reported that silty sands deposited by winds cover the Pali Aike volcanic field region. The sources of silt-sized particles are numerous in the area and include the release of particles from siltstones of the Santa Cruz Formation, aeolian abrasion of volcanic rocks under the semi-arid climate and deflation of glacial deposits accumulated in outwash plains and fans all available for wind erosion due to the scarcity of vegetation. The coarse to medium silts are typically emitted for short-term suspension transported by the impact of sand in the saltation layer (Fig. 7). They are generally deposited within ca. 30 km from the source (Muhs, 2013) but can be transported over maximum distances of tens to hundreds of km under windstorm conditions (Pye, 1995). Therefore, the MDF_{IRM} signal from the sediments of Laguna Potrok Aike primarily reflects grain-size changes of magnetite bearing silts brought to the lake by short-term suspension. This physical process implies that MDF_{IRM} likely indicates wind-intensity changes in the dust source-area of southern Argentina, with stronger winds capable of carrying coarser magnetite-bearing silts to the lake. Stronger winds are also capable of moving coarser grains by creep and saltation. These coarser grains are unlikely to reach the central lake basin; however, they can settle closer to the lake shore. This interpretation is supported by coarser grain-sizes deposited on a lake level terrace during the last glacial period (mean of 51 μm; Haberzettl et al., 2008) than at PASADO site 2 in the lake center (mean of 36 μm), as well as scanning electron microscope and energy dispersive X-ray spectroscopy (SEM–EDS) identification of iron-rich angular to sub-rounded grains typical for aeolian transport to the lake shore and sediment sequence (Supplementary material 3; Jouve et al., 2013).

5.2.2. *Possible environmental influence on MDF_{IRM}*

Other control than wind strength on magnetite bearing silts deposition would impact MDF_{IRM} values and limits its use as a wind-intensity proxy from the sedimentary sequence of Laguna Potrok Aike. Here we discuss the possible influences, including the distance from the source, presence of permafrost and vegetation, snow and ice cover, changes in lake level and sediment remobilization events.

The grain size of aeolian deposits varies inversely to the distance from the source (Fig. 7) (Pye, 1995; Muhs, 2013). For example, Sayago et al. (2001) reported a coarsening of Argentinean loess deposits from 26°S to 39°S (over 1000 km distance) inversely proportional to the distance from the Andean piedmont source area where fine clastic sediment accumulated during previous glaciations. In contrast, Laguna Potrok Aike is located only at ca. 100 km east of the Andean cordillera, within the distance range for coarse to medium silt (the fraction best correlated to MDF_{IRM}; Table 1) transport by short-term suspension (from ca. 30 km to hundreds of km; Pye, 1995; Muhs, 2013). Because of this proximity of the lake to the source, and because MDF_{IRM} values do not differ for periods of outwash plain or proglacial lakes in the region during the last glacial period and deglaciation (Sugden et al., 2009), the MDF_{IRM} record from Laguna Potrok Aike is considered mostly independent of the distance from the source.

Permafrost, snow and ice cover, as well as vegetation changes in the vicinity of the lake could potentially influence the availability of grains for aeolian transport. As MDF_{IRM} is independent of concentration change and strictly reflects the coercivity of ferrimagnetic grains, only persistent permafrost and/or snow cover blanketing the ground for extended periods of time would influence the MDF_{IRM} values by inhibiting aeolian transport to the lake and modifying the ferrimagnetic assemblage. Similarly, sustained ice cover on the lake would stop detrital input of magnetite. There is evidence of permafrost during the last Glacial period (Jouve et al., submitted for publication; Lisé-Pronovost et al., 2014; Kliem et al., 2013b) which probably contributed via increased runoff to higher lake levels (Fig. 3F). However greater values of the concentration-dependent magnetic parameters k_{LF} (Figs. 3A and 4B), ARM and IRM (Lisé-Pronovost et al., 2013) as well as similar values of Fmag (Fig. 3C) during the last Glacial period compared to the Holocene suggest that grain transport to the lake was not inhibited, but rather enhanced. This greater magnetite grain availability during the last Glacial period do not support any sustained periods of permafrost, snow cover and/or ice cover that would have impacted MDF_{IRM} at the millennial to centennial time scale; however, they may have acted discontinuously, on an annual basis or over short periods of time, possibly contributing to the high amplitude of changes in rock-magnetic properties.

One could argue that if the lake level is lowered, the distance from the shore to the coring site is reduced and coarser grains can possibly reach the coring site (Kasper et al., 2012). However, the steep slopes (up to 20°; Anselmetti et al., 2009) to the deep basin of Laguna Potrok Aike limit significant surface area changes from lake level fluctuations. In addition, there is currently no evidence that lake levels at Laguna Potrok Aike have substantially fluctuated during the last Glacial period (51,200–17,300 cal BP) (Fig. 3F). Therefore, the lake-level influence on the silt grain-size deposited in the lake center is believed to be small. During the Mid to Late Holocene, the strong SWW are persistent over the region (Zolitschka et al., 2013 and references therein), accordingly bringing distinctively coarser magnetite grains to Laguna Potrok Aike (lower values of MDF_{IRM}; Figs. 3E and 4B). Finally, the absence of MDF_{IRM} change concomitant to the ca. 35 m Late Holocene lake-level transgression (Fig. 3F) further supports the independence of MDF_{IRM} on lake-level changes.

Finally, another possible influence on the MDF_{IRM} signal is the input of silt-sized magnetite by runoff events such as after extreme precipitation (Ohlendorf et al., 2013), permafrost and snow melt, or remobilization of previously deposited coarser mud induced by lake-level changes. However, such events were recognized and removed from the event-corrected PASADO composite sediment sequence (Kliem et al., 2013a) used for this study, and, hence, do not impact the MDF_{IRM} data presented here. Altogether, the discussed possible environmental influence on grain-size deposition is unlikely to impact MDF_{IRM} at the millennial to centennial time scale.

5.2.3. Comparison of MDF_{IRM} with wind intensity records

The final step for testing the reliability of MDF_{IRM} as a wind intensity proxy is through comparison with other wind-intensity records from the Southern Hemisphere. During the last Glacial period (51,200–17,300 cal BP), the MDF_{IRM} signal from Laguna Potrok Aike indicates generally lower winds with large amplitude changes. Lower wind intensities during the last Glacial period relative to the present are in agreement with an equatorward displacement of the polar front (Iriondo, 1999; Moreno et al., 1999; Pollock and Bush, 2013; Toggweiler et al., 2006) or a weakening of the Southern Hemisphere westerly winds (Kohfeld et al., 2013), and weaker winds are also documented in the Australasian region (Shulmeister et al., 2004; Hesse and McTainsh, 1999). This pattern is interrupted by two periods of lower MDF_{IRM} (enhanced wind strength) at Laguna Potrok Aike and reduced amplitudes centered at ca. 44,000 and ca. 39,000 cal BP (Fig. 6D). These two inferred relatively stronger wind periods are coeval (within limits of respective chronologies) to enhanced wind-driven upwelling in the Pacific, Indian and Atlantic sectors of the Southern Ocean (Anderson et al., 2009; Fig. 6G) as well as to stronger winds in the mid-latitudes of the Southern Hemisphere in New Zealand (Whittaker et al., 2011; Fig. 6E) and further north offshore Namibia (Pichevin et al., 2005; Fig. 6F).

During the Late Glacial warming recorded from ca. 17,000 to 11,000 cal BP in Antarctica (EPICA Community Members, 2006) (Fig. 6H), MDF_{IRM} from Laguna Potrok Aike and paleowind records from the mid-latitudes of the Southern Hemisphere indicate increased intensities (Fig. 6D, E and G) (Anderson et al., 2009; Whittaker et al., 2011) while no change is observed further north offshore Namibia (Pichevin et al., 2005; Fig. 6F), in agreement with a poleward shift of the SWW at the last Glacial termination. The early Holocene period (ca. 11,000 to 8100 cal BP) is characterized by high amplitude changes and generally weaker winds at Laguna Potrok Aike (Fig. 8). This period corresponds to the cessation of wind-driven upwelling in the sub-polar Southern Ocean (Anderson et al., 2009; Fig. 6G) and to reduced flow across the entire zone of westerly influence from ca. 11,000 to 8000 cal BP (shaded area in Fig. 8) as reported by Fletcher and Moreno (2012 and references therein) reviewing continuous paleoenvironmental records in the mid-latitudes of the Southern Hemisphere.

Fig. 8A, C and D presents a regional comparison (within 500 km; Table 2) of MDF_{IRM} from Laguna Potrok Aike with wind intensity records in southeastern Patagonia since 14,000 cal BP (Table 2). The annual precipitation of westerly origin inferred from palynological data from Lago Argentino on the Andean piedmont (Tonello et al., 2009; Fig. 8C), as well as the sand influx to a peat bog on Terra del Fuego (Björck et al., 2012; Fig. 8D), display a similar series of maximum wind intensities (labeled from 1 to 7), providing regional support for MDF_{IRM} as a wind intensity proxy.

The mid to late Holocene period (since 8100 cal BP) is characterized by distinctively stronger wind intensities and low amplitude variability consistent with the present-day strong and persistent SWW over the region (Ohlendorf et al., 2013). The

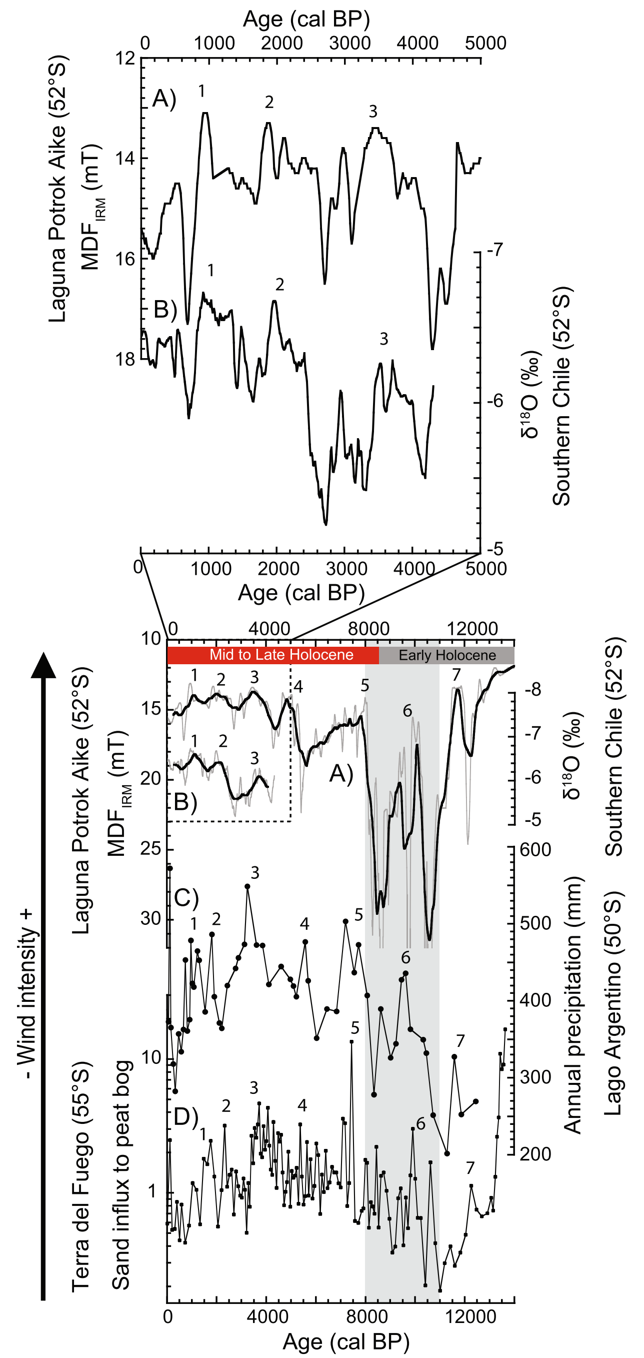

Fig. 8. Regional comparison of wind-intensity proxies for southern South America since 14,000 cal BP (Table 2). A) Median destructive field of isothermal remanent magnetization (MDF_{IRM}) from the sediment of Laguna Potrok Aike (this study), B) $\delta^{18}O$ from the stalagmite MA1 in Southern Chile (Schimpf et al., 2011), C) annual precipitation reconstruction from pollen data of Lago Argentino in southern Argentina (Tonello et al., 2009) and D) sand (125–350 μm) influx to a peat bog on Terra del Fuego (Björck et al., 2012). All records are presented on their own chronology. The thick lines represent millennial time scale variability for high-resolution records A and B. Numbers (1 to 7) indicate a series of relative maxima in wind intensity for all records. Climatic periods of the PASADO record are indicated and the shaded area indicates a period of weak westerly flow in the mid-latitudes of the Southern Hemisphere according to Fletcher and Moreno (2012).

sharp shift to stronger winds at 8100 cal BP inferred from MDF_{IRM} (Figs. 7 and 8) likely marks the onset of the SWW influence over 52°S in southeastern Patagonia, in agreement with the zonally symmetric increase in westerly flow at ca. 8000 cal BP reported by Fletcher and Moreno (2012). This period corresponds to major environmental changes in Laguna Potrok Aike

Table 2
Dust and wind intensity proxies from the Southern Hemisphere discussed in the text.

Proxy	Site position				Age (cal BP)		References
	Site	Distance from LPA (km)	Latitude	Longitude	min	max	
Dust							
Magnetic susceptibility (k) of marine sediments	Scotia Sea	1780	58°S	42°W	0	92,500	Weber et al., 2012
Flux of dust to ice core	EPICA Dome C, Antarctica	5870	75°06′S	123°24′E	0	62,000	Lambert et al., 2012
Wind intensity							
$\delta^{18}O$ from stalagmite (MA1)	Bahia Arevalo, southern Chile	220	52°41′S	73°23′W	0	4500	Schimpf et al., 2011
Annual precipitation reconstructed from pollen data	Lago Argentino, southern Argentina	240	50°24′S	72°42′W	0	12,400	Tonello et al., 2009
Eolian sand influx in peat bog	Isla de los Estados, Tierra del Fuego	500	54°45′S	64°30′W	0	14,000	Björck et al., 2012
Opal flux to marine sediment cores TN057-13	Atlantic sector of the Southern Ocean	4940	52°06′S	5°06′E	0	27,000	Anderson et al., 2009
"TN057-14"		4910	51°59′S	4°31′E	22,000	82,000	Anderson et al., 2009
Coarse grain size fraction mode of marine sediment	Off-shore Namibia	7450	25°06′S	13°38′E	0	190,000	Pichevin et al., 2005
$\delta^{18}O$ from stalagmite (HW3)	Hollywood cave, New Zealand	8020	41°57′S	171°28′E	11,000	73,000	Whittaker et al., 2011

including low lake levels (Anselmetti et al., 2009; Haberzettl et al., 2007; Kliem et al., 2013b), palynological evidence of decreased precipitation (Schäbitz et al., 2013), and increased Andean forest taxa brought by westerly winds (Mayr et al., 2007a; Wille et al., 2007), diminution of total diatom-valve abundance and changes in taxonomical assemblages (Massaferro et al., 2013), as well as monohydrocalcite precipitation (Haberzettl et al., 2007; Nuttin et al., 2013). Marked landscape changes including peat-growth termination by aeolian sand deposition and dune developments are also reported at that time on the West Falkland Island ca. 600 km east of Laguna Potrok Aike (Wilson et al., 2002).

Finally, the record from Laguna Potrok Aike is compared with a high-resolution wind intensity record derived from $\delta^{18}O$ of a stalagmite on the western side of the Andean cordillera since 5000 cal BP (Schimpf et al., 2011) (Fig. 8A and B). The two records are located only 220 km apart at 52°S under the influence of the strong SWW. Despite contrasting climate (hyperhumid in southern Chile and dry steppe in southern Argentina), the records are in agreement at a centennial time scale, implying that since 5000 cal BP, stronger SWW was associated to increased precipitation in southwestern Patagonia and to coarser magnetite bearing grains transported over southeastern Patagonia. Altogether, regional to hemispheric comparisons of wind-intensity proxies and well-established high-resolution paleoclimate data from the Southern Hemisphere provide support for interpreting the MDF_{IRM} record from Laguna Potrok Aike as a wind-intensity proxy in southeastern Patagonia, at least at the millennial time scale and up to the centennial time scale during the mid to late Holocene.

5.2.4. Summary

The proposed wind intensity control on magnetite bearing silt sizes deposited in Laguna Potrok Aike through time is supported by the paleoenvironmental context in southeastern Patagonia and a similar signal variability to various types of regional and Southern Hemisphere wind intensity proxies. One significant advantage of MDF_{IRM} as a wind intensity proxy is its ability to target mostly the magnetite grains of a specific grain-size range. Such a narrow grain-size target facilitates identification of the transport process. In addition, MDF_{IRM} is not influenced by changes in magnetic concentration (as opposed to k_{LF}) or by changes in the various sediment types and grain sizes of the bulk sediment. Moreover, because winds in southeastern Patagonia are only weakly related to precipitation (Garreaud et al., 2013; Ohlendorf et al., 2013), MDF_{IRM} is believed to be independent of moisture changes. This is a significant advantage for southern Patagonia where the moisture-related wind-intensity proxies are often difficult to interpret (Moreno et al., 2009) particularly during times of rearrangements of the hydrological cycle such as during deglaciation (Kohfeld et al., 2013).

6. Conclusions

High-resolution rock-magnetic studies of the sediment deposited in the maar lake Laguna Potrok Aike since 51,200 cal BP revealed a lacustro-aeolian record in the dust source-region of southern Patagonia. The magnetic susceptibility signal (k_{LF}) displays a very clear LGM signal (from 31,500 to 17,300 cal BP), not provided by most other proxies from Laguna Potrok Aike. There is an inverse correlation of k_{LF} with ferrimagnetic coercivity and grain-size indicators (e.g., MDF_{IRM}, kARM/IRM) at the millennial to centennial time scale. On longer time scale however, the variability of k_{LF} appears primarily controlled by the concentration of ferrimagnetic minerals. Based on coherence analysis, estimation of magnetite flux to the lake and comparison with distal dust records, k_{LF} is interpreted as a dust proxy in the dust source-region of southern Patagonia at the multi millennial time scale, where ferrimagnetic coercivity and grain size influence is minimal.

This study established the MDF_{IRM} record from Laguna Potrok Aike as a wind intensity proxy in southeastern Patagonia since 51,200 cal BP. The coercivity of the magnetite grains acquiring an isothermal remanent magnetization (MDF_{IRM}) tracks the wind-blown magnetite-bearing coarse to medium silts transported by short-term suspension. The new wind-intensity proxy, independent of moisture change, is in agreement with other wind-intensity records derived from marine, lacustrine and peat bog sediments, as well as from speleothems in southern Patagonia since deglaciation and from the Southern Hemisphere during the last Glacial period.

Acknowledgements

We acknowledge J. Labrie, F. Barletta, M.-P. St-Onge and D. Veres for their help in the laboratory at ISMER. We are grateful to two anonymous reviewers for constructive comments on the manuscript as well as A. Chauvin and J. Stoner for reading an earlier draft. Thanks to A. Mazaud and Q. Simon for fruitful discussions and to S. Björck, A. Hahn, P. Kliem, F. Lambert, L. Pichevin, D. Schimpf, M. Tonello, M. Weber and T. Whittaker for sharing their data. This research was supported by the International Continental scientific Drilling Program (ICDP expedition 5022). Funding for drilling was provided by the ICDP, the German Research Foundation (DFG DFG Zo 102/11-1, 2), the Swiss National Funds (SNF 200020-119931 and 200020-119931/2), the Natural Sciences and Engineering Research Council of Canada (NSERC 5796-352379-2007), the Swedish Research Council (VR 2006-5868) and the University of Bremen (PASADO-University of Bremen-2). For their invaluable help in field logistics and drilling, we thank the staff of INTA Santa Cruz and Rio Dulce Catering as well as the Moreteau family and the DOSECC crew. This research was made possible through a NSERC Special Research Opportunity and Discovery grants to G. St-Onge and P. Francus. We also acknowledge the Canadian Foundation for Innovation (CFI 10738) for the acquisition and operation of the u-channel cryogenic magnetometer. Finally, we acknowledge the support of NSERC and the Canadian Meteorological and Oceanographical Society (CMOS) for graduate scholarships to A. Lisé-Pronovost, and the *Fonds de recherche du Québec – Nature et technologies* (FQRNT) for a postdoctoral fellowship to T. Haberzettl.

Appendix A. Supplementary material

Supplementary material related to this article can be found online at http://dx.doi.org/10.1016/j.epsl.2014.11.007.

References

Anderson, R.F., et al., 2009. Wind-driven upwelling in the Southern Ocean and the deglacial rise in atmospheric CO_2. Science 323 (5920), 1443–1448.
Anselmetti, F., et al., 2009. Environmental history of southern Patagonia unraveled by the seismic stratigraphy of Laguna Potrok Aike. Sedimentology 56, 873–892.
Banerjee, S.K., et al., 1981. A rapid method for magnetic granulomtery with applications to environmental studies. Geophys. Res. Lett. 8, 333–336.
Basile, I., et al., 1997. Patagonian origin of glacial dust deposited in East Antarctica (Vostok and Dome C) during glacial stages 2, 4 and 6. Earth Planet. Sci. Lett. 146, 573–589.
Björck, S., et al., 2012. Multi-proxy analyses of a peat bog on Isla de los Estados, easternmost Tierra del Fuego: a unique record of the variable Southern Hemisphere Westerlies since the last deglaciation. Quat. Sci. Rev. 42, 1–14.
Brachfeld, S.A., 1999. Separation of geomagnetic paleointensity and paleoclimate signals in sediments: examples from North America and Antarctica. PhD thesis. University of Minnesota.
Cisowski, S., 1981. Interacting vs. non-interacting single domain behavior in natural and synthetic samples. Phys. Earth Planet. Inter. 26, 56–62.
Coronato, A., et al., 2013. Glacial, fluvial and volcanic landscape evolution in the Laguna Potrok Aike maar area, Southern Patagonia, Argentina. Quat. Sci. Rev. 71, 13–26.
Dankers, P., 1981. Relationship between median destructive field and remanent coercive forces for dispersed natural magnetite, titanomagnetite and hematite. Geophys. J. R. Astron. Soc. 64, 447–461.
Day, R., et al., 1977. Hysteresis properties of titano-magnetite: grain size and compositional dependence. Phys. Earth Planet. Inter. 13, 260–267.
Dearing, J.A., 1999. Environmental Magnetic Susceptibility: Using the Bartington MS2 System. Chi Pub., Kenilworth. 54 p.
Delmonte, B., et al., 2004. Comparing the Epica and Vostok dust records during the last 220,000 years: stratigraphical correlation and provenance in Glacial periods. Earth-Sci. Rev. 66, 63–87.
Delmonte, B., et al., 2010. Geographic provenance of aeolian dust in East Antarctica during Pleistocene glaciations: preliminary results from Talos Dome and comparison with East Antarctic and new Andean ice core data. Quat. Sci. Rev. 29, 256–264.
D'Orazio, M., et al., 2000. The Pali Aike volcanic field, Patagonia: slab-window magmatism near the tip of South America. Tectonophysics 321, 407–427.
Dunlop, D.J., 2002. Theory and application of the Day plot (Mrs/Ms versus Hcr/Hc). Theoretical curves and tests using titanomagnetite data. J. Geophys. Res. 107 (B3), 1–22.
Dunlop, D.J., Özdemir, Ö., 1997. Rock Magnetism, Fundamentals and Frontiers. Cambridge Studies in Magnetism Series. Cambridge University Press. 573 p.
Dunlop, D.J., Özdemir, Ö., 2007. Magnetizations in rocks and minerals. In: Schubert, G. (Ed.), Geomagnetism, Treatise on Geophysics, vol. 5. Elsevier, pp. 277–336.
Egli, R., 2004. Characterization of individual rock magnetic components by analysis of remanence curves. Phys. Chem. Earth, Parts ABC 29, 851–867.
EPICA Community Members, 2006. One-to-one coupling of glacial climate variability in Greenland and Antarctica. Nature 444, 195–198.
Evans, M., Heller, F., 2003. Environmental Magnetism: Principles and Applications of Enviromagnetics. International Geophysics Series, vol. 86. Academic Press, p. 299.
Fletcher, M.-S., Moreno, P.I., 2012. Have the Southern Westerlies changed in a zonally symmetric manner over the last 14,000 years? A hemisphere-wide take on a controversial problem. Quat. Int. 253, 32–46.
Gaiero, D.M., 2007. Dust provenance in Antarctic ice during glacial periods: from where in southern South America? Geophys. Res. Lett. 34, L17707.
Garreaud, R., et al., 2013. Large scale control on the Patagonia climate. J. Climate 26, 215–230.
Gogorza, C.S.G., et al., 2011. Paleosecular variation andpaleointensity records for the last millennium from southern South America (Laguna Potrok Aike, Santa Cruz, Argentina). Phys. Earth Planet. Inter. 184, 41–50.
Gogorza, C.S.G., et al., 2012. High-resolution paleomagnetic records from Laguna Potrok Aike (Patagonia, Argentina) for the last 16,000 years. Geochem. Geophys. Geosyst. 13 (12), Q12Z37.
Haberzettl, T., et al., 2005. Climatically induced lake level changes during the last two millennia as reflected in sediments of Laguna Potrok Aike, southern Patagonia (Santa Cruz, Argentina). J. Paleolimnol. 33, 283–302.
Haberzettl, T., et al., 2007. A continuous 16,000 year sediment record from Laguna Potrok Aike, southern Patagonia (Argentina): sedimentology, chronology, geochemistry. Holocene 17, 297–310.
Haberzettl, T., et al., 2008. Hydrological variability in southeastern Patagonia and explosive volcanic activity in the southern Andean Cordillera during Oxygen Isotope Stage 3 and the Holocene inferred from lake sediments of Laguna Potrok Aike, Argentina. Palaeogeogr. Palaeoclimatol. Palaeoecol. 259, 213–229.
Haberzettl, T., et al., 2009. Late Pleistocene dust deposition in the Patagonian steppe – extending and refining the paleoenvironmental and tephrochronological record from Laguna Potrok Aike back to 55 ka. Quat. Sci. Rev. 28, 2927–2939.
Hahn, A., et al., 2013. Climate induced changes as registered in inorganic and organic sediment components from Laguna Potrok Aike (Argentina) during the past 51 ka. Quat. Sci. Rev. 71, 154–166.
Hahn, A., et al., 2014. Elemental composition of the Laguna Potrok Aike sediment sequence reveals paleoclimatic changes over the past 51 ka in southern Patagonia, Argentina. J. Paleolimnol. http://dx.doi.org/10.1007/s10933-014-9798. Published online October 7th, 2014.
Heider, F., et al., 1996. Magnetic susceptibility and remanence coercive force in grown magnetite crystals from 0.1 mm to 6 mm. Phys. Earth Planet. Inter. 93, 239–256.
Hesse, P.P., McTainsh, G.H., 1999. Last Glacial maximum to Early Holocene wind strength in the mid-latitudes of the Southern Hemisphere from aeolian dust in the Tasman Sea. Quat. Res. 52, 343–349.
Hjulström, F., 1935. Studies of the morphological activity of rivers as illustrated by the river Fyris. In: University of Uppsala Geological Institute Bulletin, vol. 25, pp. 221–557.
Iriondo, M.H., 1999. Last glacial maximum and hypsithermal in the Southern Hemisphere. Quat. Int. 62, 11–19.
Irurzun, M.A., et al., 2014. Magnetic parameters and their palaeoclimatic implications – the sediment record of the last 15 500 cal BP from Laguna Potrok Aike (Argentina). Geophys. J. Int. http://dx.doi.org/10.1093/gji/ggu155. Published online June 2, 2014.
Jouve, G., et al., 2013. Microsedimentological characterization using image analysis and μ-XRF as indicators of sedimentary processes and climate changes during Lateglacial at Laguna Potrok Aike, Santa Cruz, Argentina. Quat. Sci. Rev. 71, 191–204.
Jouve, G., et al., submitted for publication. Microsedimentological investigations in lacustrine sediments from a maar lake: implications for paleoenvironmental reconstructions. J. Paleolimnol.
Kasper, T., et al., 2012. Indian Ocean Summer Monsoon (IOSM)-dynamics within the past 4 ka recorded in the sediments of Lake Nam Co, central Tibetan Plateau (China). Quat. Sci. Rev. 39, 73–85.
Kilian, R., Lamy, F., 2012. A review of Glacial and Holocene paleoclimate records from southernmost Patagonia (49–55°S). Quat. Sci. Rev. 53, 1–23.
King, J., et al., 1982. A comparison of different magnetic methods for determining the relative grain size of magnetite in natural materials: some results from lake sediments. Earth Planet. Sci. Lett. 59, 404–419.
Kliem, P., et al., 2013a. Lithology, radiocarbon chronology and sedimentological interpretation of the lacustrine record from Laguna Potrok Aike, southern Patagonia. Quat. Sci. Rev. 71, 54–69.
Kliem, P., et al., 2013b. Magnitude, geomorphologic response and climate links of lake level oscillations at Laguna Potrok Aike, Patagonian steppe (Argentina). Quat. Sci. Rev. 71, 131–146.
Kohfeld, K.E., et al., 2013. Southern Hemisphere westerly wind changes during the Last Glacial Maximum: paleo-data synthesis. Quat. Sci. Rev. 68, 76–95.
Kok, J.F., 2011. Does the size distribution of mineral dust aerosols depend on the wind speed at emission? Atmos. Chem. Phys. 11, 10149–10156.
Kruiver, P.P., et al., 2001. Quantification of magnetic coercivity components by the analysis of acquisition curves of isothermal remanent magnetisation. Earth Planet. Sci. Lett. 189, 269–276.

Lambert, F., et al., 2012. Centennial mineral dust variability in high-resolution ice core data from Dome C, Antarctica. Climacteric 8, 609–623.

Lamy, F., et al., 2010. Holocene changes in the position and intensity of the southern westerly wind belt. Nat. Geosci. 3, 695–699.

Lisé-Pronovost, A., et al., 2013. High-resolution paleomagnetic secular variations and relative paleointensity since the Late Pleistocene in southern South America. Quat. Sci. Rev. 71, 91–108.

Lisé-Pronovost, A., et al., 2014. Rock-magnetic signature of precipitation and extreme runoff events in south–eastern Patagonia since 51,200 cal BP from the sediments of Laguna Potrok Aike. Quat. Sci. Rev. 98, 110–125.

Lisiecki, L.E., Raymo, M.E., 2005. A Plio-Pleistocene stack of 57 globally distributed benthic d18O records. Paleoceanography 20.

Liu, Q., et al., 2012. Environmental magnetism: principles and applications. Rev. Geophys. 50.

Lowrie, W., Fuller, M., 1971. On the alternating field demagnetization characteristics of multidomain thermoremanent magnetisation in magnetite. J. Geophys. Res. 76 (26), 6339–6349.

Maher, B.A., 1988. Magnetic properties of some synthetic submicron magnetites. Geophys. J. 94, 83–96.

Maher, B.A., 2011. The magnetic properties of Quaternary aeolian dusts and sediments, and their palaeoclimatic significance. Aeolian Res. 3, 87–144.

Maher, B.A., Thompson, R., 1999. Quaternary Environments, Climates and Magnetism. Cambridge University Press. 390 p.

Maher, B.A., et al., 2010. Global connections between aeolian dust, climate and ocean biogeochemistry at the present day and at the last glacial maximum. Earth-Sci. Rev. 99, 61–97.

Massaferro, J., et al., 2013. Major lake level fluctuations and climate changes for the past 16,000 years as reflected by diatoms and chironomids preserved in the sediment of Laguna Potrok Aike, southern Patagonia. Quat. Sci. Rev. 71, 167–174.

Mayr, C., et al., 2007a. Holocene variability of the Southern Hemisphere westerlies in Argentinean Patagonia (52S). Quat. Sci. Rev. 26, 579–584.

Mayr, C., et al., 2007b. Precipitation origin and evaporation of lakes in semi-arid Patagonia (Argentina) inferred from stable isotopes (d18O, d2H). J. Hydrol. 334, 53–63.

Mayr, C., et al., 2013. Intensified Southern Hemisphere Westerlies regulated atmospheric CO_2 during the last deglaciation. Geology 41, 831–834.

Mazaud, A., et al., 2007. Variations of the ACC-CDW during MIS3 traced by magnetic grain deposition in midlatitude South Indian Ocean cores: connections with the northern hemisphere and with central Antarctica. Geochem. Geophys. Geosyst. 8 (5), Q05012.

Mazaud, A., et al., 2010. Variations of the Antarctic Circumpolar Current intensity during the past 500 ka. Geochem. Geophys. Geosyst. 11 (8), Q08007.

McGee, D., et al., 2010. Gustiness: the driver of glacial dustiness? Quat. Sci. Rev. 29, 2340–2350.

Moreno, P.I., et al., 1999. Abrupt vegetation and climate changes during the last glacial maximum and last termination in the Chilean Lake District: a case study from Canal de la Puntilla (41°S). Geogr. Ann., Ser. A 81A, 285–311.

Moreno, P.I., et al., 2009. Millennial-scale variability in Southern Hemisphere westerly wind activity over the last 5000 years in SW Patagonia. Quat. Sci. Rev. 28, 25–38.

Moreno, P.I., et al., 2012. Deglacial changes of the southern margin of the southern westerly winds revealed by terrestrial records from SW Patagonia (52°S). Quat. Sci. Rev. 41, 1–21.

Moskowitz, B.M., 1991. Hitchhiker's guide to magnetism. In: Enviromental Magnetism Workshop. 48 p.

Moy, C.M., et al., 2008. Isotopic evidence for hydrologic change related to the westerlies in SW Patagonia, Chile, during the last millennium. Quat. Sci. Rev. 27, 1335–1349.

Muhs, D.R., 2013. The geologic records of dust in the Quaternary. Aeolian Res. 9, 3–48.

Nuttin, L., et al., 2013. Authigenic, detrital and diagenetic minerals in the Laguna Potrok Aike sediment sequence. Quat. Sci. Rev. 71, 109–118.

Ohlendorf, C., et al., 2013. Mechanisms of lake-level change at Laguna Potrok Aike (Argentina) – insights from hydrological balance calculations. Quat. Sci. Rev. 71, 27–45.

Paillard, D., et al., 1996. Macintosh program performs time-series analysis. Eos Trans. AGU 77, 379.

Peters, C., Dekkers, M.J., 2003. Selected room temperature magnetic parameters as a function of mineralogy, concentration and grain size. Phys. Chem. Earth, Parts ABC 28, 659–667.

Petit, J.R., et al., 1999. Climate and atmospheric history of the past 420,000 years from the Vostok ice core, Antarctica. Nature 399, 429–436.

Pichevin, L., et al., 2005. A 190 ky record of lithogenic grain-size on the Namibian slope: forging a tight link between past wind-strength and coastal upwelling dynamics. Mar. Geol. 218, 81–96.

Pollock, E.W., Bush, A.B.G., 2013. Atmospheric simulations of southern South America's climate since the Last Glacial maximum. Quat. Sci. Rev. 71, 219–228.

Pugh, R.S., et al., 2009. Circum-Antarctic age modelling of Quaternary marine cores under the Antarctic Circumpolar Current: ice-core dustemagnetic correlation. Earth Planet. Sci. Lett. 284, 113–123.

Pye, K., 1995. The nature, origin and accumulation of loess. Quat. Sci. Rev. 14, 653–667.

Recasens, C., et al., 2012. New insights into paleoenvironmental changes in Laguna Potrok Aike, Southern Patagonia, since the Late Pleistocene: the PASADO multiproxy record. Holocene 22, 1323–1335.

Roberts, A.P., et al., 2011. Atmospheric dust variability from Arabia and China over the last 500,000 years. Quat. Sci. Rev. 30, 3537–3541.

Ross, P.-S., et al., 2011. Influence of the substrate on maar–diatreme volcanoes: an example of a mixed setting from the Pali Aike volcanic field, Argentina. J. Volcanol. Geotherm. Res. 201, 253–271.

Röthlisberger, R., 2002. Dust and sea salt variability in central East Antarctica (Dome C) over the last 45 kyrs and its implications for southern high-latitude climate. Geophys. Res. Lett. 29 (20), 1963.

Sayago, et al., 2001. Genesis and distribution of the Late Pleistocene and Holocene loess of Argentina: a regional approximation. Quat. Int. 76/77, 247–257.

Schäbitz, F., et al., 2013. Reconstruction of palaeoprecipitation based on pollen transfer functions – the record of the last 16 ka from Laguna Potrok Aike, southern Patagonia. Quat. Sci. Rev. 71, 175–190.

Schaefer, J.M., et al., 2006. Near-synchronous interhemispheric termination of the last glacial maximuminmid-latitudes. Science 312, 1510–1513.

Schimpf, D., et al., 2011. The significance of chemical, isotopic, and detrital components in three coeval stalagmites from the superhumid southernmost Andes (53°S) as high-resolution palaeo-climate proxies. Quat. Sci. Rev. 30, 443–459.

Shulmeister, J., et al., 2004. The Southern Hemisphere westerlies in the Australasian sector over the last glacial cycle: a synthesis. Quat. Int. 118–119, 23–53.

Sijp, W.P., England, M.H., 2008. The effect of a northward shift in the southern hemisphere westerlies on the global ocean. Prog. Oceanogr. 79, 1–19.

St-Onge, G., et al., 2007. Continuous physical properties of cored marine sediments. In: Hillaire-Marcel, C., DeVernal, A. (Eds.), Developments in Marine Geology. Elsevier, pp. 63–98.

Stoner, J.S., St-Onge, G., 2007. Magnetic stratigraphy in paleoceanography: reversals, excursions, paleointensity, and secular variation. In: Hillaire-Marcel, C., DeVernal, A. (Eds.), Developments in Marine Geology. Elsevier, pp. 99–138.

Stoner, J.S., et al., 1996. The magnetic signature of rapidly deposited detrital layers from the deep Labrador Sea: relationship to North Atlantic Heinrich layers. Paleoceanography 11 (3), 309–325.

Sugden, D.E., et al., 2009. Influence of Patagonian glaciers on Antarctic dust deposition during the last glacial period. Nat. Geosci. 2, 281–285.

Tauxe, L., 2010. Essentials of Paleomagnetism. University of California Press, Berkeley. 489 p.

Thompson, R., 1986. Palaeomagnetic dating. In: Berglund, B.E. (Ed.), Handbook of Holocene Palaeoecology and Palaeohydrology. Wiley, Chichester, UK, pp. 313–327.

Toggweiler, J.R., et al., 2006. Midlatitude westerlies, atmospheric CO_2, and climate change during the ice ages. Paleoceanography 21.

Tonello, M.S., et al., 2009. Quantitative reconstruction of Holocene precipitation changes in southern Patagonia. Quat. Res. 72, 410–420.

Tucker, M.E., 2001. Sedimentary Petrology: An Introduction to the Origin of Sedimentary Rocks. Blackwell Science Publications, Cambridge. 272 p.

Udden, J.A., 1914. Mechanical composition of clastic sediments. Bull. Geol. Soc. Am. 25, 655–744.

Vandenberghe, J., 2013. Grain size of fine-grained windblown sediment: a powerful proxy for process identification. Earth-Sci. Rev. 121, 18–30.

Villa-Martinez, R., Moreno, P.I., 2007. Pollen evidence for variations in the southern margin of the westerly winds in SW Patagonia over the last 12,600 years. Quat. Res. 68, 400–409.

Vuillemin, A., et al., 2013. Origin and significance of diagenetic concretions in sediments of Laguna Potrok Aike, southern Argentina. J. Paleolimnol. 50, 275–291.

Waldmann, N., et al., 2010. Holocene climatic fluctuations and positioning of the Southern Hemisphere westerlies in Tierra del Fuego (54°S), Patagonia. J. Quat. Sci. 25 (7), 1063–1075.

Weber, M.E., et al., 2012. Dust transport from Patagonia to Antarctica – a new stratigraphic approach from the Scotia Sea and its implications for the last glacial cycle. Quat. Sci. Rev. 36, 177–188.

Wentworth, C.K., 1922. A scale of grade and class terms for clastic sediments. J. Geol. 30, 377–392.

Whittaker, T.E., et al., 2011. Abrupt millennial-scale changes in intensity of Southern Hemisphere westerly winds during marine isotope stages 2–4. Geology 39, 455–458.

Wille, M., et al., 2007. Vegetation and climate dynamics in southern South America: the microfossil record of Laguna Potrok Aike, Santa Cruz, Argentina. Rev. Palaeobot. Palynol. 146, 234–246.

Wilson, P., et al., 2002. Late Pleistocene and Holocene landscape evolution and environmental change in the Lake Sulivan area, Falkland Islands, South Atlantic. Quat. Sci. Rev. 21, 1821–1840.

Xu, S., Dunlop, D.J., 1995. Toward a better understanding of the Lowrie-Fuller test. J. Geophys. Res., Solid Earth 100 (B11), 22533–22542.
Zolitschka, B., et al., 2006. Crater lakes of the Pali Aike Volcanic Field as key sites for paleoclimatic and paleoecological reconstructions in southern Patagonia, Argentina. J. South Am. Earth Sci. 21, 294–309.
Zolitschka, B.F., et al., 2009. The Laguna Potrok Aike Scientific Drilling Project PASADO (ICDP Expedition 5022). Sci. Drill. 8, 29–33.
Zolitschka, B., et al., 2013. Environment and climate of the last 51,000 years – new insights from the Potrok Aike maar lake Sediment Archive Drilling prOject (PASADO). Quat. Sci. Rev. 71, 1–12.